Antal Kerpely Doctoral School of Materials Science and Technology

Synthesis of Metal Oxides Nanoparticles by Precipitation-Calcination Method and their Application for CO_2 Capture from Air

Thesis Booklet

By

EI EI KHINE

Master of Science (Physics), Taunggyi University, Myanmar

Supervisors:

Prof. Dr. George Kaptay, Professor

Prof. Dr. Peter Baumli, Professor

Head of the Doctoral School

Prof. Dr. Valéria Mertinger

Institute of Physical Metallurgy, Metal Forming and Nanotechnology
Faculty of Materials and Chemical Engineering
University of Miskolc
Miskolc, Hungary

2022

1.Introduction

Nanoparticles (NPs) are a group of materials made up of small particles that have at least one dimension less than 100 nm. Many research works have been reported regarding the uses of different metal oxide nanoparticles. Al_2O_3 nanoparticles have been suggested to enhance the mechanical properties of cement[1]. Fe_3O_4, TiO_2, CuO, and ZnO were reported as potential candidates for antibacterial agents [2]. Metal oxide nanoparticles can be used as antimicrobial agents, prospective drug delivery agents, and in various other biomedical applications.

The metal oxide nanoparticles can be produced by using various methods such as sol-gel [3–5], thermal decomposition [6–8], hydrothermal technique, combustion method, co-precipitation technique [9-10], biogenic method, precipitation method, two-step thermal decomposition technique, one step multi-component synthesis [11], microwave synthesis [12] and sonication method [13]. The metal oxide nanoparticles can be used to capture CO_2 [14].

Among the nanometal oxide, CaO nanoparticles can be used as an antimicrobial agent, a potential drug delivery agent, as well as in various other biomedical applications. CaO is an interesting CO_2 absorber, owing to its excellent kinetics and substantial capturing efficiency, even at weak CO_2 concentration environment [15–21].

Hence, this study aims to optimize sustainable sorbent efficiency in long-term capturing applications. Several techniques can be utilized to prepare CaO nanoparticles; the chemical and physical characteristics of CaO can be modified at the nano level. Morphology, surface area and capturing efficiency can be carefully managed under precise synthesis environments and favorably influence the sorbents' reactivity [22-25].

2. Literature Review

1.1 Synthesis of metal oxide nanoparticles

Metal oxide nanoparticles have been produced from different reagents by different synthesis techniques, including precipitation, combustion, sol-gel, wet chemical, microwave, mechanochemical, and hydrolysis. CaO [26-27], CoO/Co_3O_4[28], CuO[29] and ZnO[30] have been produced by using precipitation method from metal chlorides and NaOH. CoO nanoparticles have been produced only at very high temperatures, and the produced nanoparticles are only stable in the unoxidized environment. CoO transformed to Co_3O_4 in air [31].

Knowledge gap: There is no study describing the possible candidates of metal oxide nanoparticles can be synthesized through the precipitation-calcination method from metal chloride and NaOH.

As a theoretical approach, the possibility of producing metal oxides will be calculated through precipitation-calcination method in this research.

2.2 Metal oxides nanoparticles for CO_2 capturing

FeO, Fe_2O_3 and Fe_3O_4 iron oxides have been investigated for CO_2 capturing process [32]. KO_2 transforms to K_2CO_3 in water and CO_2 environment [33]. However, BeO nanotube has been used for CO_2 absorption [34-35]. Li_2O transformed to Li_2CO_3 under CO_2 environment at low temperatures; this decarbonation process works at 600 °C [36- 37]. MgO

particles have been produced for carbonation at room temperature to 316 °C [38]. Na_2O has better CO_2 absorption ability than Li_2O and K_2O for the MgO absorbent of carbon capturing [39]. Among those metal oxides (M = Mg, Ca, K, Na), MgO has less CO_2 absorption capacity compared to CaO, K_2O and Na_2O. The carbonation process of MgO was done at 25 - 100 °C [40 - 41]. NiO particles have the capability for carbonation- decarbonation process when it is done at low temperatures [42]. ZnO particles have the capability for carbonation-decarbonation process when the carbonation process is done at a temperature range of 25 - 100 °C in air, under flowing CO_2 gas. Moreover, decarbonation process of ZnO was done at 250 - 300 °C [43 - 44].

Knowledge gap: The missing information is the potential applications of metal oxide nanoparticles for CO_2 capturing.

2.3 The synthesis of CaO nanoparticles and the characterizations

Few research groups have reported the synthesis routes of CaO nanoparticles by thermal decomposition, combustion method, sol-gel, hydrothermal technique, co-precipitation technique, biogenic method, two-step thermal decomposition technique, and microwave synthesis. Generally, CaO nanoparticles are often produced via the thermal treatment of $Ca(OH)_2$ [45]. CaO nanoparticles are produced by the decomposition of $CaCO_3$ at a high temperature greater than 900 °C [46] or by precipitation method using different reagents [47]. Calcium oxide (CaO) nanoparticles were synthesized by the sol-gel method [48]. Two researchers produced CaO nanoparticles by using $CaCl_2$ and NaOH reagents through precipitation- calcination process. The calcination process was done in the N_2 environment. The produced CaO samples are in the sub-micron scales.

Knowledge gap: The missing information is the possibility of producing CaO nanoparticles by calcination in air. Moreover, to produce 100 % pure CaO and small particle size (below 100 nm) could be considered.

2.4 Enhancing the properties of CaO by doping using different metal oxides

Doping the CaO nanoparticles with various atoms is recognized as an essential way to boost the capturing effectiveness and the stability of the sorbent materials [49]. Several research studies have been done that exhibit superior characteristics of metal-doped CaO nanoparticles. ZrO_2 doped to CaO was conducted to increase the sorption of CO_2 [50]. Iron(III) oxide and cobalt doped to CaO are used for the preparation of composite materials [51 –53]. Fe ion-doped CaO was investigated at low-temperature conditions below 700 °C as a catalyst to absorb CO_2. Iron is an excellent element to improve both the catalytic activity and the carbon deposition in catalytic examinations. The reaction of Fe_2O_3 and CaO has enhanced the properties of CaO [54].

Knowledge gap: There is no study to describe the characterizations of the metal oxides doped CaO nanoparticles through precipitation-calcination method.

2.5 Absorption of CO_2 by CaO nanoparticles

The use of calcium-based sorbents for CO_2 absorption is primarily done through capture/regeneration loops of CaO utilizing the following reaction: $CaO + CO_2 = CaCO_3$. The capturing operation is a chemical process. Generally, at 650 °C under ambient pressure,

CO_2, CaO, and $CaCO_3$ are formed in the process. To increase the performance of CaO-based sorbents, several approaches have been suggested, including pore structure manipulation and new metal doping.

Knowledge gap: (i) The missing information is that is it possible to capture CO_2 at low temperatures? (ii) Moreover, can metal oxide-doped CaO nanoparticles control the stability of CO_2 capturing at low temperatures?

3. Theoretical calculation of the metal oxide synthesis through the precipitation-calcination method

As an example, the synthesis of CaO nanoparticles by adding NaOH solution dropwise to $CaCl_2$ solution and forming $Ca(OH)_2$ precipitates, and after washing-filtering it to calcine it to form CaO. This was done to capture CO_2 with the formation of $CaCO_3$. Firstly, NaOH is indeed a suitable reagent. The calculation of the following steps is based on the CRC Handbook of Chemistry and Physics [55] and Barin Thermochemical Data of Pure Substances [56].

3.1 Condition 1. Existence and solubility of a stable chloride for a given metal

The reaction takes place between an aqueous solution of the metal chloride (MCl_x) and NaOH. The first condition is whether the given metal has a stable chloride and whether its solubility in water is sufficient. To be sufficient, the solubility should be larger than the planned concentration. The planned concentration should be taken in stoichiometry with 2 M NaOH. Thus, for MCl_x, the required solubility,

$$s_{r(MClx)} = 2/x\ M \qquad \text{Eq 3.1-1}$$

Where S_r = required solubility in molarity (M), x = the positive integer.

But the solubility given in g/100g of H_2O, the unit can be recalculated to the unit of molarity (M).

$$s_{a(M)(MClx)} = s_{a(g)MClx} * 10 / M_{MClx} \qquad \text{Eq 3.1-2}$$

Where, $s_{a(M)(MClx)}$ = the actual solubility of metal chloride with unit molarity M, $s_{a(g)MClx}$ = actual solubility of metal chloride with unit g/100 g of H_2O, M_{MClx} = molar mass of metal chloride with unit g/mol.

Those metal metal chlorides are listed that have sufficient solubility for this technology: M = Al, Au (III), Ba, Be, Ca, Cd, Co (II), Cs, Cu (II), Fe (III), Fe (II), In (III), K, La, Li, Mg, Mn (II), Na, Nd, Ni (II), Pr, Pt (IV), Rb, Sb (III), Sm (III), Sn (II), Sr, Y, Zn. These are altogether 29 chlorides for 29 metals. The metals which do not obey condition 1 are: M = Ag (I), Au (I), Cu (I), Hg (I), Hg (II), Pb (II), Ra, Tl (I). These metals are excluded for further consideration.

3.2 Condition 2. Spontaneous reaction between metal chloride and NaOH

The reaction is written as:

$$MCl_x + x\ NaOH = x\ NaCl + M(OH)_x \qquad \text{Eq 3.2-1}$$

Where MCl_x = metal chloride, x = positive integer, $M(OH)_x$ = metal hydroxide. This reaction will be spontaneous if the standard molar Gibbs energy change accompanying this reaction is as negative as possible. As there are (1+x) moles on both sides of the above reaction, the

concentration ratio of $M(OH)_x$ / MCl_x is the (1+ x) root of the equilibrium constant of reaction 3.2.1. To have a sufficient driving force for this reaction, which is needed for fast reaction and that is needed for fast nucleation and that is needed for nanostructure, at least 100 should be the ratio of concentrations $M(OH)_x$ / MCl_x. So, the equilibrium constant of reaction (3.2-1) should be $K = 100^{1+x}$. From here, the standard Gibbs energy change of reaction (3.2-1) should be more negative than the following value.

$$\Delta_r G^0_{required} = -4.61RT(1+x) \quad \text{Eq 3.2-2}$$

where, $\Delta_r G^0_{required}$ = the required Gibbs free energy value for the reaction with unit kJ/mol, R = gas constant value with unit $Jmol^{-1}K^{-1}$, T= Temperature with unit kelvin K.

The Gibbs energy change of reaction of metal chloride to metal hydroxide is

$$\Delta_{r1} G^0 = (\Delta_f G^0_{M(OH)x} - \Delta_f G^0_{MClx}) \quad \text{Eq 3.2-3}$$

The Gibbs energy change of reaction of NaOH to NaCl is

$$\Delta_{r2} G^0 = (\Delta_f G^0_{NaOH} - \Delta_f G^0_{NaCl}) \quad \text{Eq 3.2-4}$$

The calculation of Gibbs free energy value for the reaction 3.2-1 is;

$$\Delta_{r3} G^0 = \Delta_{r1} G^0 - x\Delta_{r2} G^0 \quad \text{Eq 3.2-5}$$

where, $\Delta_{r1} G^0$, $\Delta_{r2} G^0$, $\Delta_{r3} G^0$ = Gibbs free energy value for the reaction with unit kJ/mol, $\Delta_f G^0_{M(OH)x}$= the standard molar Gibbs energy of formation of metal hydroxide with unit kJ/mol, $\Delta_f G^0_{MClx}$ = the standard molar Gibbs energy of formation of metal chloride with unit kJ/mol, $\Delta_f G^0_{NaOH}$ = the standard molar Gibbs energy of formation of NaOH with unit kJ/mol, $\Delta_f G^0_{NaCl}$ = the standard molar Gibbs energy of formation of NaCl with unit kJ/mol.

The metals are listed for this condition 2 is also obeyed from the above list of 29 chlorides (for which condition 1 is obeyed): M = Al, Au (III), Ba, Be, Ca, Cd, Co (II), Cu (II), Fe (III), Fe (II), Li, Mg, Mn (II), Ni (II), Sb (III), Sn (II), Sr, Zn = 18 chlorides for 18 metals. The metals which do obey condition 1 but do not obey condition 2 are: M = Cs, In (III), K, La, Na, Nd, Pr, Pt (IV), Rb, Sm (III), Y. These metals are excluded for further consideration.

3.3 Condition 3. Fast precipitation of metal hydroxide

The metal hydroxide formed in the previous step should precipitate fast in order to form nano crystallite. For that, the solubility of metal hydroxide should be much lower than actual concentration. The concentration of metal hydroxide is maximum about 1/x M (supposing the same volume of NaOH solution is added to the same volume of metal chloride solution). To make sure the precipitation is fast, it is required at least 10 times less solubility, i.e., below 0.1/x M.

$$s_{(required)M(OH)x} = 0.1/x \text{ M} \quad \text{Eq 3.3-1}$$

Where, $s_{(required)M(OH)x}$ = the required solubility of metal hydroxides with unit molarity M.

The unit should be recalculated to molarity. But the solubility of metal hydroxides given in g/100g of H_2O, the unit can be recalculated to the unit of molarity (M).

$$s_{a(M)(M(OH)x)} = s_{a(g)M(OH)x} * 10 / M_{M(OH)x}$$

where, $s_{a(M)(M(OH)x)}$ = the actual solubility of metal hydroxide with unit molarity M, $s_{a(g)M(OH)x}$ = actual solubility of metal hydroxide with unit g/100 g of H_2O, $M_{M(OH)x}$ = molar mass of metal hydroxide with unit g/mol.

Those metals which obey this condition and their hydroxides are expected to precipitate quickly: M = Al, Au (III), Be, Ca, Cd, Co (II), Cu (II), Fe (III), Fe (II), Mg, Mn (II), Ni (II), Sb (III), Sn (II), Zn = 15 hydroxides of 15 metals. The metals which do obey condition 2 but do not obey condition 3 are: M= Ba, Li, Sr.

3.4 Condition 4. Ability of metal hydroxide to convert into metal oxide upon heating

The following chemical reaction is expected:

Case I : if x = even (2,4,6,….)

$$M(OH)_x = \frac{x}{2} H_2O + MO_{\frac{x}{2}} \quad \text{Eq 3.4-1}$$

Case II : if x = odd (1,3,5,….)

`

$$2\ M(OH)_x = x\ H_2O + M_2O_x \quad \text{Eq 3.4-2}$$

For x = 2 we can write: $M(OH)_2 = H_2O + MO$. As the only gaseous component of the reaction equation, 3.4-1 is on the right-hand side; this reaction will be shifted to the right with increasing temperature. Therefore, it is expected that at least some of the hydroxides will thermally decompose at a higher temperature. This reaction should take place spontaneously, preferably without using vacuum, at a reasonably low temperature, meaning at least below half of the melting point of metal oxide, denoted as T*, T_m is Tammann temperature T_T. Meanwhile, T_T is the same as the decomposition temperature of metal hydroxide. This should be obeyed, as above this temperature, the nanoparticles will easily sinter and lose their nanostructure. The decomposition temperature of equation 3.4-1 is known. Moreover, the decomposition temperature should be in a reasonable engineering range, not above 1500 K.

From those which obeyed this condition and using the technology: chloride + NaOH = hydroxide + NaCl + washing + precipitation of hydroxide + calcination leading to an oxide, we can obtain the following 13 oxides: M = Al, Be, Ca, Cd, Co (II), Cu (II), Fe (III), Fe (II), Mg, Mn (II), Ni (II), Sn (II), Zn = 13 oxides of 13 metals. The metals which do not obey this condition: Au (III), Sb (III).

3.5 Additional Condition: CO_2 capturing efficiency of the metal oxide produced by the precipitation-calcination method

All the above is done in order to produce an oxide that is able to capture CO_2, according to the reaction:

Case I: if x = even (2,4, 6….)

$$MO_{\frac{x}{2}} + \frac{x}{2} CO_2 = M(CO_3)_{\frac{x}{2}} \quad \text{Eq 3.5-1}$$

Case II: if x = odd (1,3, 5….)

$$M_2O_x + x\ CO_2 = M_2(CO_3)_x \quad \text{Eq 3.5-2}$$

where, $MO_{\frac{x}{2}}$, M_2O_x = metal oxides, $M(CO_3)_{\frac{x}{2}}$, $M_2(CO_3)_x$ metal carbonates.

If x = 2, reaction 3.5-1 simplifies as: $MO + CO_2 = MCO_3$. As in the reaction, the gaseous component is on the left-hand side; this reaction will be shifted to the left with increasing T. Thus, let us check the possibility of this reaction at T = 300 K. If it does not work at T = 300 K, it will not work at higher temperatures, either.

The current concentration of CO_2 in the atmosphere is 420 ppm. To call a capturing technology efficient, it should decrease this value by 10 times. Thus, reaction equation 3.5-1 should have an equilibrium at a partial pressure of CO_2 of 42 ppm, i.e., p = 4.2 E-5 bar. Thus, the equilibrium constant of reaction 3.5.1 should be at least the inverse of this value to the power of K = 2/x: $(2.38\ E4)^{2/x}$ at least at T = 300 K.

Thus, the standard molar Gibbs energy change accompanying reaction 3.5.1 and 3.5.2 is; Case I: if x = even (2,4, 6….)

$$\Delta_{r4}G^0 = \Delta_f G^0_{M(CO3)_{\frac{x}{2}}} - (\Delta_f G^0_{MO_{\frac{x}{2}}} + \frac{x}{2}\Delta_f G^0_{CO2}) \quad \text{Eq 3.5-3}$$

Case II: if x = odd (1,3, 5….)

$$\Delta_{r5}G^0 = \Delta_f G^0_{M_2(CO3)_x} - (\Delta_f G^0_{M_2O_x} + x\Delta_f G^0_{CO2}) \quad \text{Eq 3.5-4}$$

where, $\Delta_{r2}G^0$, $\Delta_{r3}G^0$ = the standard molar Gibbs energy change accompanying reaction with unit kJ/mol, $\Delta_f G^0_{M(CO3)_{\frac{x}{2}}}$, $\Delta_f G^0_{M_2(CO3)_x}$ = the standard molar Gibbs energies of formation of metal carbonates with unit kJ/mol, $\Delta_f G^0_{MO_{\frac{x}{2}}}$, $\Delta_f G^0_{M_2O_x}$= the standard molar Gibbs energies of formation of metal oxides with unit kJ/mol, $\Delta_f G^0_{CO2}$ = the standard molar Gibbs energies of formation of CO_2 with unit kJ/mol.

The metal oxides which also satisfy this condition: M = Ca, Cd, Co (II), Mn (II), i.e., the following oxides (i) can be produced using our technology and at the same time (ii) they are able to capture CO_2. In sequence from the strongest to the weakest: CaO, MnO, CdO, CoO. So, the best is CaO. FeO, MgO, ZnO and NiO are weaker in reaction for carbonation. Al_2O_3, BeO, CuO, Fe_2O_3 and SnO do not obey for carbonation.

4. Materials and methods

4.1Materials and synthesis of pure metal oxide nanoparticles

$CaCl_2xH_2O$ (≥95%, Sigma Aldrich), $CoCl_2xH_2O$ (≥99%, VWR Ltd.), $FeCl_3xH_2O$ (≥95%, Sigma Aldrich), $NiCl_2xH_2O$ (≥99%, VWR Ltd.), and NaOH (≥98%, VWR Ltd.) were used as a reactant for the preparation of the samples. 1M concentration of $CaCl_2$, $CoCl_2$, $FeCl_3$, $NiCl_2$ and 2M concentration of NaOH were prepared by using distilled water.

The preparations of the pure metal oxides CaO, CoO/Co_3O_4, Fe_2O_3 and NiO are described. Each metal chloride and NaOH were used as initial reagents for the synthesis of $M(OH)_2$ powder. First, both aqueous solutions (MCl_x and NaOH) were heated up to 80 °C separately. At this fixed temperature, a given NaOH solution was added dropwise to a given MCl_x solution under stirring (1300 rpm) by a magnetic stirrer for 30 minutes. The process takes place according to the following reaction:

$$MCl_{x(aq)} + xNaOH_{(aq)} \rightarrow M(OH)_{x(s)} + xNaCl_{(aq)} \quad \text{Eq 4.1-1}$$

As a result, the precipitates were formed. After that, the mixtures were filtered and washed five times with 120ml distilled water per occasion to remove NaCl from the suspension. $M(OH)_{x(s)}$ occurred in the reactions:

$$M(OH)_{x(s)} + xNaCl_{(aq)} + nH_2O \rightarrow nH_2O + xNaCl_{(aq)} / M(OH)_{x(s,wet)} \quad \text{Eq 4.1-2}$$

The wet precipitates of $M(OH)_x$ were dried in air at room temperature for one night to collect a semi-dry precipitate $M(OH)_x$. The collected semi-dry precipitate of $M(OH)_x$ calcined

in air in the furnace with a heating rate of 15 °C/min. As a result, metal oxides CaO, CoO/Co_3O_4, Fe_2O_3 and NiO powder were produced by calcination while the dissociation product H_2O was evaporated, as shown in the following equation:

Case I: if x = even (2,4, 6….)

$$M(OH)_{x(s)} \rightarrow MO_{\frac{x}{2}} + \frac{x}{2}H_2O \uparrow \quad \text{Eq 4.1-3}$$

Case II: if x = odd (1,3, 5….)

$$2M(OH)_{x(s)} \rightarrow M_2O_x + xH_2O \uparrow \quad \text{Eq 4.1-4}$$

4.2 Synthesis of metal oxides doped CaO nanoparticles

In this section, the synthesis of three metal oxides CoO, Fe_2O_3 and NiO doped calcium oxides nanoparticles are described. In the synthesis, 0.1:1 ratio of doping MCl_x to $CaCl_2$ was used to obtain $M(OH)_2$:$Ca(OH)_2$ powder. To prepare high doping amount 0.5:1 MCl_x to $CaCl_2$ was used in the reaction with NaOH.

The initial reagents $CoCl_2$/ $NiCl_2$/$FeCl_3$, $CaCl_2$ and NaOH solutions were synthesized to produce metal oxides CoO, Fe_2O_3 and NiO doped CaO nanoparticles. First, all of the aqueous solutions ($CoCl_2$ /$NiCl_2$ /$FeCl_3$, $CaCl_2$ and NaOH) were heated up to 80 °C. At that fixed temperature, a given NaOH solution was added dropwise to the mixture of $CoCl_2$ + $CaCl_2$, $NiCl_2$ + $CaCl_2$ and $FeCl_3$ + $CaCl_2$ solution under stirring at 1300 rpm by a magnetic stirrer for 30 minutes. During the wet synthesis process, a light color precipitate for low doping precipitate and dark color precipitate for high doping precipitate was formed. The chemical reaction is as follows:

$$zMCl_{x(aq)} + CaCl_2 + (2+zx)\,NaOH_{(aq)} \rightarrow zM(OH)_{x(s)} + Ca(OH)_{2(s)} + (2+zx)\,NaCl_{(aq)} \quad \text{Eq 4.2-1}$$

where z = 0.1, 0.5 doping amount (mole/ 1 mole of $CaCl_2$) for $NiCl_2$ and $CoCl_2$, z = 0.05, 0.25 doping amount (mole/ 1 mole of $CaCl_2$) for $FeCl_3$, x = positive integer.

After that, the mixture was filtered and washed five times with 100- 150 ml of distilled water per occasion to remove NaCl from the suspension. The duration of each filtering process was 2-3 hr. The precipitates occurred according to the reactions:

$$M(OH)_x\text{: } Ca(OH)_{2(s)} + NaCl_{(aq)} + H_2O \rightarrow \begin{cases} H_2O + NaCl_{(aq)} \text{ (passed the filter)} \\ M(OH)_x\text{: } Ca(OH)_{2(\text{wet solid})} \text{ (filtered wet precipitate)} \end{cases} \quad \text{Eq 4.2-2}$$

The wet precipitate of $z(Co(OH)_2$:$Ca(OH)_2$, $Ni(OH)_2$:$Ca(OH)_2$ and $Fe(OH)_3$:$Ca(OH)_2)$ were dried in air at room temperature over one night to collect a semi-dry precipitate $z(Co(OH)_2$:$Ca(OH)_2$, $Ni(OH)_2$:$Ca(OH)_2$ and $Fe(OH)_3$:$Ca(OH)_2)$.

As a result, 0.1CoO:CaO, 0.5CoO:CaO, 0.1NiO:CaO, 0.5NiO:CaO and $0.05Fe_2O_3$:CaO, $0.25Fe_2O_3$:CaO powder were produced. H_2O, which is formed by dissociation was evaporated as shown in the following equation:

Case I: if x = even (2,4, 6….)

$$zM(OH)_x\text{:}Ca(OH)_{x(s)} \rightarrow zMO_{\frac{x}{2}}\text{:}CaO_{(s)} + (\frac{zx}{2} + 1)H_2O \uparrow \quad \text{Eq 4.2-3}$$

Case II: if x = odd (1,3, 5….)

$$zM(OH)_x\text{:}Ca(OH)_{x(s)} \rightarrow \frac{z}{2}M_2O_x\text{:}CaO_{(s)} + (\frac{zx}{2} + 1)H_2O \uparrow \quad \text{Eq 4.2-4}$$

Pure CaO and (low-doped and highly doped) metal oxides to CaO (CoO:CaO, NiO:CaO, Fe_2O_3:CaO) are measured mass increasing for the absorption capacity for CO_2 capturing. In the process, the produced samples (after the calcination of the samples) were kept at each temperature 0, 25, 50, 75, 100, 200 ºC for about 3-6 weeks. The process of measuring the mass increase for each sample has been done every day until the mass becomes maximum. While the samples are saturated for CO_2 capturing.

5. Results and discussions

5.1 Crystallite sizes of metal oxides nanoparticles produced by the precipitation-calcination method

XRD analysis confirmed that pure CaO powder with 80 nm of crystallite size is detected as seen in Figure 5.1-1 that has cubic crystallite lattice system. XRD diffractograms show only the existence of Co_3O_4 i.e; CoO transformed into Co_3O_4 in the oxidizing environment. CoO phase is only at high temperature, that transformed into Co_3O_4 when it was cooled down, which is a stable phase. The crystallite size of Co_3O_4 is 17 nm as seen in Figure 5.1-2 and it has a hexagonal crystallite lattice system. Figure 5.1-3 shows Fe_2O_3 (hematite) with 16 nm of crystallite size. Figure 5.1-4 shows XRD diffractogram of NiO with 30 nm of the crystallite size. Moreover, the other researchers produced CuO and ZnO through the same routes using metal chloride and NaOH with the crystallite size in sub-micro and nanoscale. Furthermore, BeO, NiO, MgO, and SnO have been produced using metal chlorides and NaOH through different routes

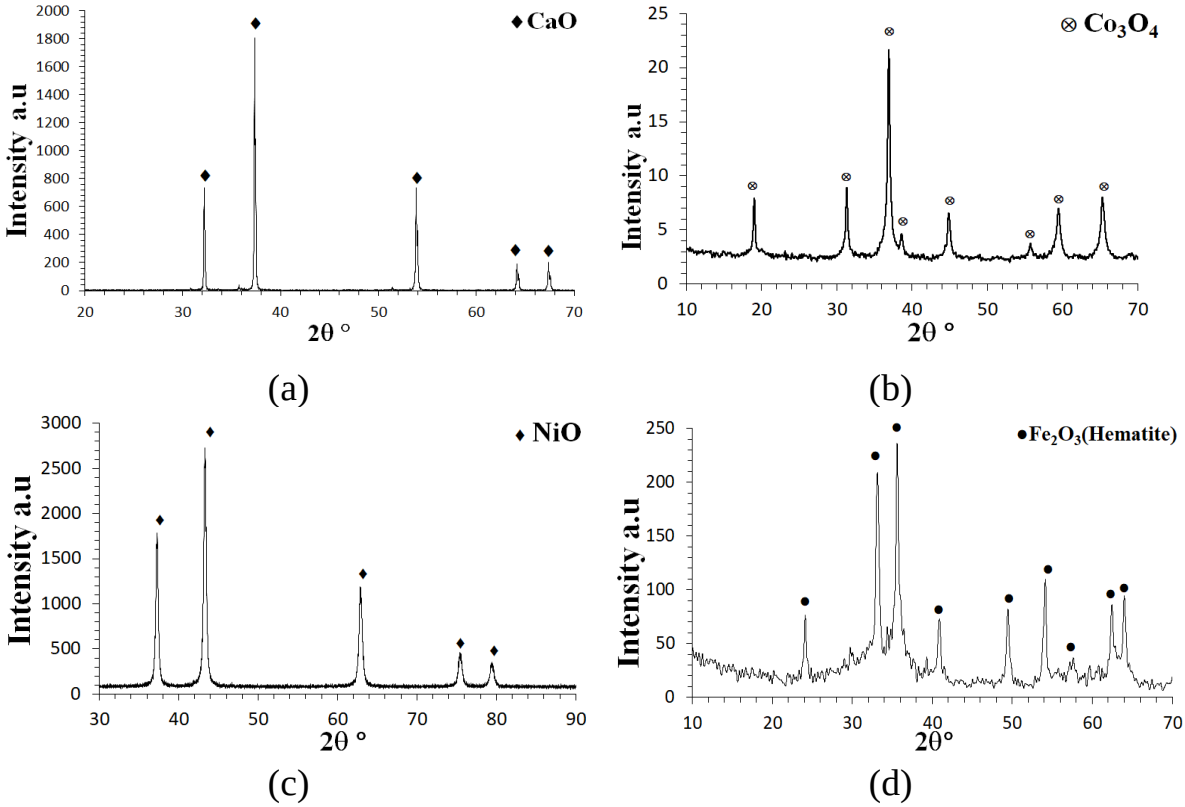

Figure 5.1: XRD pattern of (a) CaO from dry precipitate $Ca(OH)_2$ (b) Co_3O_4 from dry precipitate $Co(OH)_2$ (c) Fe_2O_3 from dry precipitate $Fe(OH)_3$ (d) NiO from dry precipitate $Ni(OH)_2$ that the dry precipitates were calcined in air.

5.2 Crystallite sizes of CaO nanoparticles

The wet precipitates $Ca(OH)_2$ were calcined under vacuum and in air at the temperature range of 25 - 650 °C in the chamber of the XRD. Figure 5.2 a show a series of XRD diffractograms of sample 1(calcination under vacuum). It follows that the initial wet precipitate at 25 ºC contains mostly $Ca(OH)_2$ with very few amounts of $CaCO_3$. The peaks for $Ca(OH)_2$ disappeared in the temperature range between 250 and 300 ºC; instead, new peaks of CaO appeared and remained stable till the maximum measured temperature of 650 ºC. The small peak of $CaCO_3$ disappeared in the temperature range between 500 and 550 ºC. Similar results of sample 2 (calcination in air) are shown in Figure 5.2 b for the case when the in-situ calcination in the XRD equipment was performed in air. Compared to Figure 5.2 b, calcination in air (instead of vacuum) leads to prolonged stability by about 150 ºC for both initial compounds: from 300 to 450 ºC for $Ca(OH)_2$ and from 500 to 650 ºC for $CaCO_3$. This is due to the high entropy of the gaseous reaction products H_2O and CO_2 that drives the dissociation reaction in a vacuum further and faster compared to the case when calcination is performed in air.

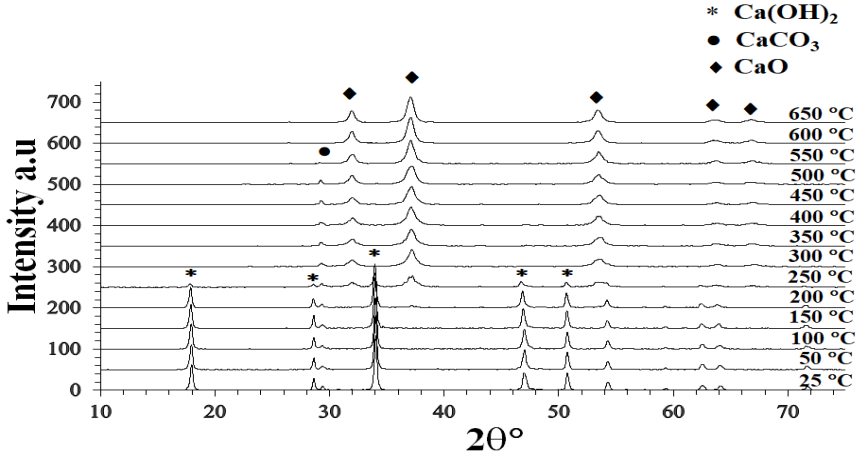

(a)

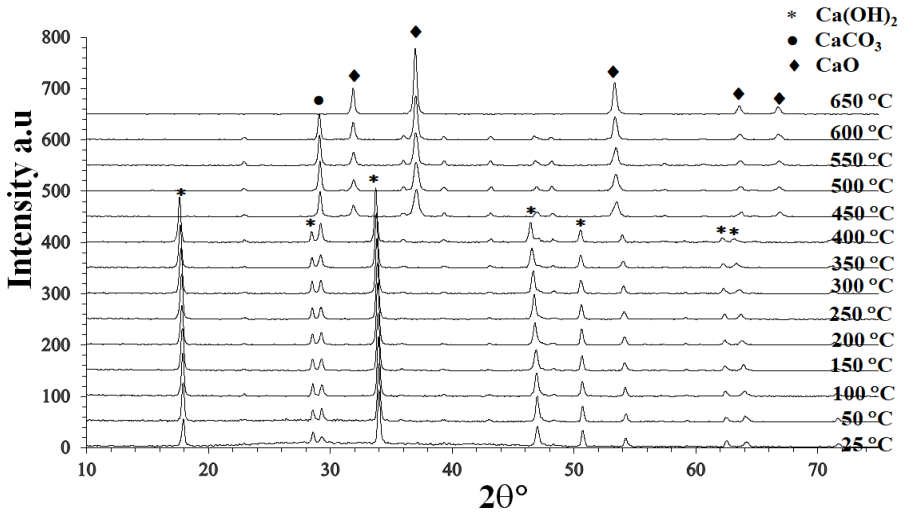

(b)

Figure 5.2: XRD diffractograms of CaO during its calcination steps in the temperature range of 25 - 650 ºC(a) calcination under vacuum (b) calcination in air

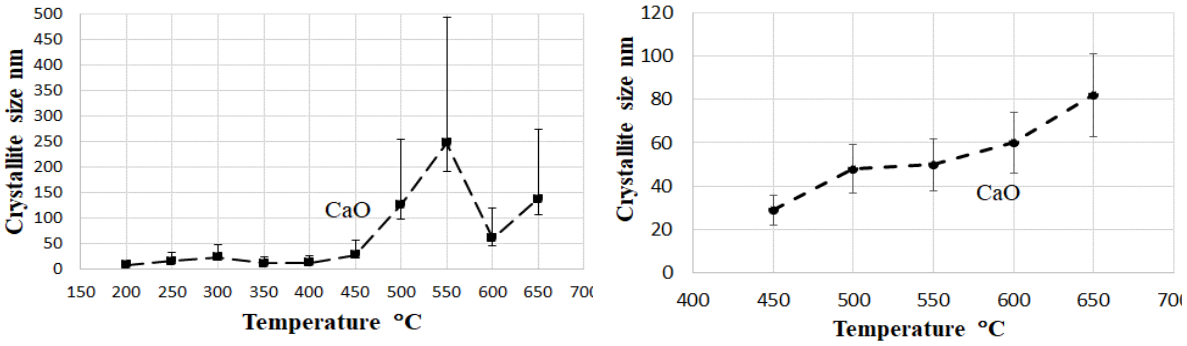

(a) (b)

Figure 5.3: The crystallite sizes of CaO as a function of temperatures in the range of 50 - 650 °C (a) calcination under vacuum (b) calcination in air

5.3: XRD investigation of metal oxides doped CaO nanoparticles.

XRD characterization of three different metal oxides CoO, NiO and Fe_2O_3 doped CaO; each doping sample was prepared based on the ratio 0.1: 1 and 0.5:1 of MCl_x $CoCl_2$, $NiCl_2$, $FeCl_3$ to $CaCl_2$ during the reactions. The calcination temperature of all doped CaO samples is 650 ºC.

In low-doped CaO samples, 0.1CoO:CaO sample has two phases CaO and $Ca_2Co_2O_5$, with crystallite sizes of 105 and 50 nm. 0.1NiO:CaO sample has two phases CaO and NiO, with the crystallite sizes 50 nm. 0.05Fe_2O_3:CaO sample has three phases CaO, Fe_2O_3 and $Ca_2Fe_2O_5$, with crystallite sizes of 165, 808, 14 nm, respectively, as seen in Figure 5.4.

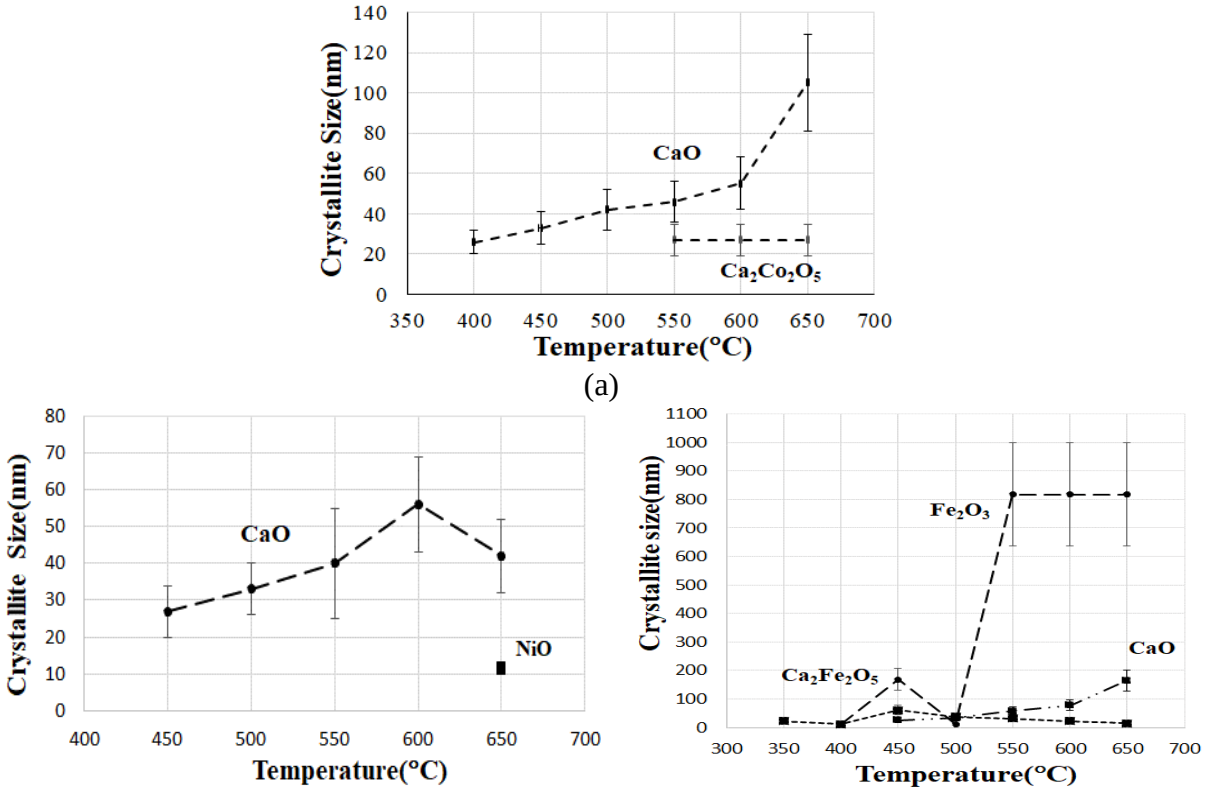

(a)

(b) (c)

Figure 5.4: The crystallite sizes of (a) 0.1CoO:CaO (b) 0.1NiO:CaO and (c) 0.05Fe_2O_3:CaO prepared from 0.1:1 mole ratio of MCl_x to $CaCl_2$ by wet precipitate calcined in air 25-650 ºC measured at each 50 ºC.

In highly doped CaO samples, 0.5CoO:CaO sample has three phases CaO, CoO and $CaCo_2O_4$, with crystallite sizes of 65, 23 and 19 nm, respectively. 0.5NiO:CaO sample has two phases CaO and NiO with crystallite sizes of 198 and 45 nm. 0.05Fe_2O_3:CaO sample has three phases CaO and $Ca_2Fe_2O_5$ with crystallite sizes of 818 and 30 nm, as seen in Figure 5.5.

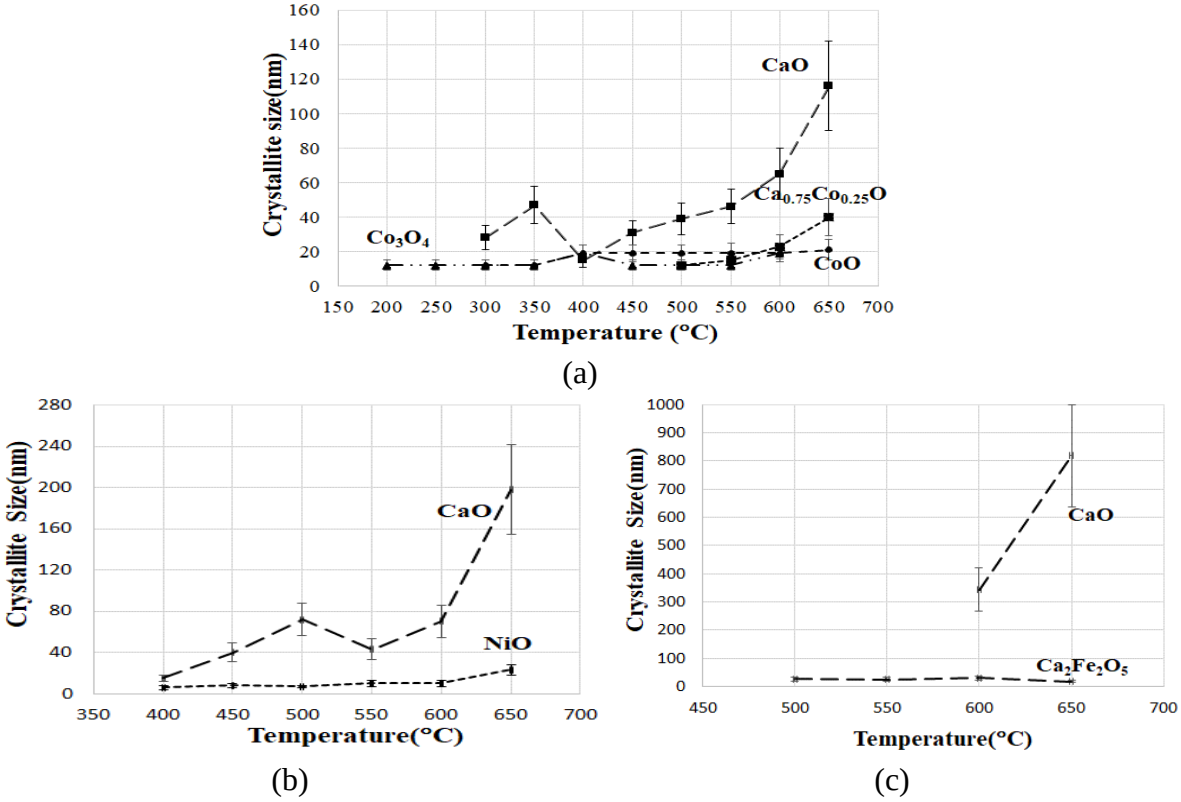

Figure 5.5: The crystallite sizes of (a) 0.5CoO:CaO (b) 0.5NiO:CaO and (c) 0.25Fe_2O_3:CaO prepared from 0.5:1 mole ratio of MCl_x to $CaCl_2$ by wet precipitate calcined in air 25-650 ºC measured at each 50 ºC.

5.4 Absorption capacity and specific surface areas of pure CaO and metal oxides doped CaO.

Figure 5.6 and Figure 5.7 show the maximum capturing efficiency of pure CaO with low-doped and highly-doped CaO nanoparticles as a function of measured temperatures. Regarding the graph, CaO has a high capturing capacity.

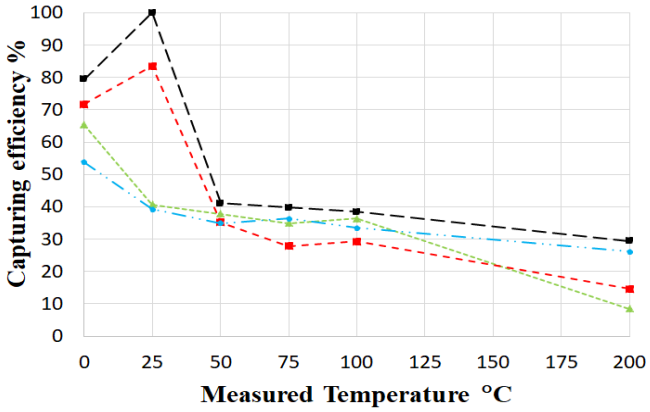

Figure 5.6: The maximum capturing capacity (%) of pure CaO and 0.1CoO:CaO, 0.1NiO:CaO and 0.05Fe_2O_3:CaO at different measured temperatures.

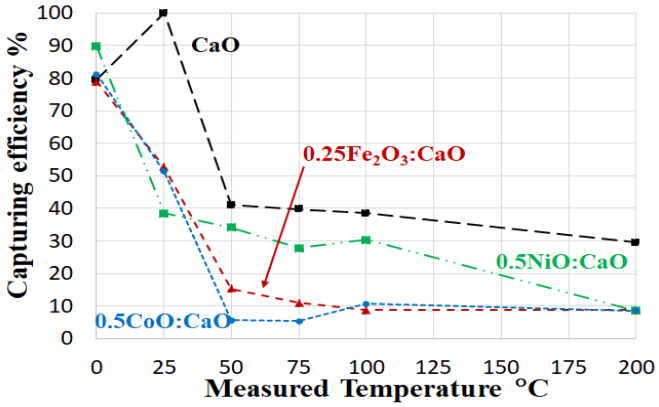

Figure 5.7: The maximum capturing capacity (%) of pure CaO and 0.5CoO:CaO, 0.5NiO:CaO and 0.25Fe_2O_3:CaO at different measured temperatures.

6. Claims

In this work, aqueous solutions of different metal chlorides (for example, calcium chloride) were mixed with an aqueous solution of NaOH at 80 °C. As a result, usually solid crystalline metal hydroxide (for example, calcium hydroxide) precipitates from the solution and the side product NaCl remains dissolved in it. The precipitates were collected by filtering and washed by water to decrease their NaCl contamination. Then, the samples were dried overnight and calcined to obtain metal oxide particles (for example, calcium oxide). These metal oxide particles appeared to be nano-sized, or at least sub-micron sized. These metal oxide samples were kept in normal air at different temperatures for several weeks to measure their mass increase, indicating capture of some carbon dioxide from air by the formation of metal carbonate (for example, calcium carbonate). In this work, the structure and phase composition of the synthesized nano-metal-oxide samples are measured before and after carbonization as a function of synthesis conditions and conditions of carbon dioxide capture. Additionally, a model is made to understand and predict the processes better.

Claim 1: Theoretical results

1.1. Selection of of useful metal chloride to prepare nano-metal-oxides. All existing stable solid metal chlorides were analyzed using mostly thermodynamic data from literature to select those metals, whose nano-metal-oxides can be produced from their metal chlorides with reasonable efficiency by the method described above. The criteria considered are as follows: (i) sufficient solubility of the given metal chloride in water, (ii) sufficient ability of the given metal chloride to convert into metal hydroxide by 1 M NaOH, (iii) low enough solubility of the given metal hydroxide in water to ensure its fast precipitation, (iv) reasonably low calcination temperature at which the given metal hydroxide can be converted into the desired metal oxide ensuring its nano-structure. It is claimed here that the following 13 nano-metal-oxides can be produced by the above-described method: Al_2O_3, BeO, CdO, CaO, CoO/Co_3O_4, CuO, FeO, Fe_2O_3, MgO, MnO, NiO, SnO and ZnO (note: CoO is primarily produced but if calcination is performed in air, then CoO is oxidized to Co_3O_4). These theoretical results are confirmed by literature data on experimental findings.

1.2. Selection of nano-metal-oxides from the above list that can capture carbon dioxide from air reducing its content 10-fold. The 13 metal oxides listed in Claim 1.1 are theoretically tested for their ability to capture carbon dioxide from air under standard temperature lowering the partial pressure of carbon dioxide from its present average value in our environment of 420 ppm to the target value of 42 ppm. The result is (in order of their decreasing ability to capture carbon dioxide): CaO, MnO, CdO, Co_3O_4. Additionally, FeO, MgO, ZnO and NiO are found as possible candidates for partial carbon dioxide capture, but they cannot lower the current carbon dioxide content in air 420 ppm to the target value of 42 ppm.

Claim 2. Effect of calcination environment (vacuum or air) on CaO nano-particles

CaO nanoparticles were prepared from wet $Ca(OH)_2$ precipitates by calcination during 1 hour between 25 and 650 °C in two different environments: vacuum and air (vacuum is a usual method in the literature, air is the novel and simple method).

2.1. Transformation temperature. It is shown that the temperature of full transformation of $Ca(OH)_2$ into CaO is lower when calcination is performed in vacuum 600 °C, as seen in Figure C1 compared when it is transformed in air 650 °C, as seen in Figure C1 b. This is due to the high entropy of the gaseous reaction product H_2O that drives the dissociation reaction in vacuum further and faster compared to the case when calcination is performed in air.

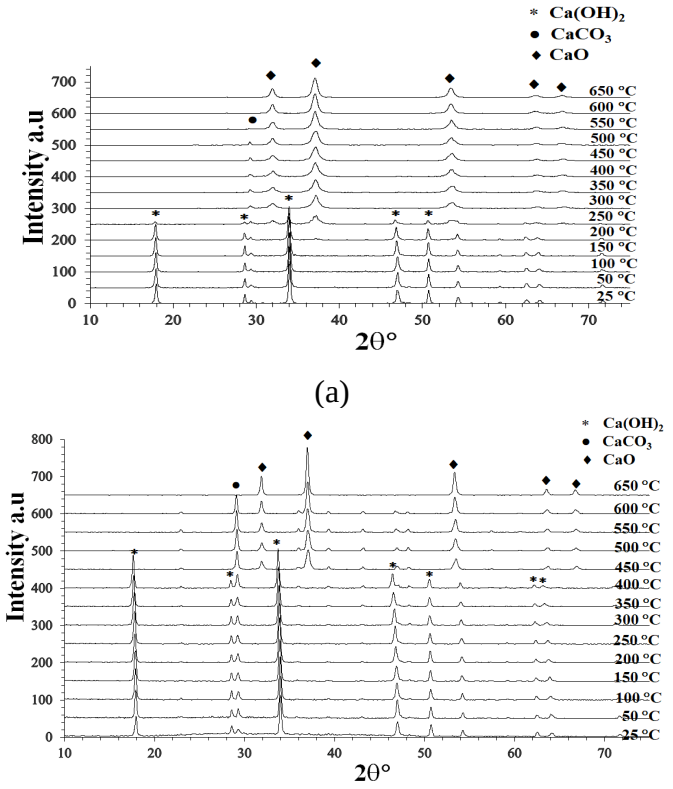

Figure C1: XRD diffractograms of CaO during its calcination steps in the temperature range of 25 - 650 ºC(a) calcination under vacuum (b) calcination in air

2.2. Recrystallization upon calcination. The crystallite sizes of CaO nano-particles calcined under vacuum go through a maximum at 550 °C due to their recrystallization to eliminate lattice defects and dislocations, as seen in Figure C2a. However, this maximum is not present for the case when CaO was obtained by calcination in air, as in this case, CaO is not re-crystallized, as seen in Figure C2.b.

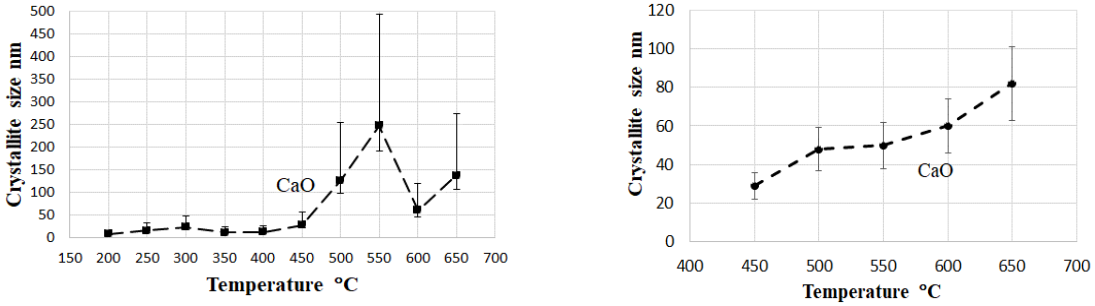

(a) (b)

Figure C2. The crystallite sizes of CaO as a function of temperatures in the range of 50 - 650 °C (a) calcination under vacuum (b) calcination in air

2.3. Final sizes after after calcination at 650 °C. The final crystallite sizes of CaO nano-particles obtained after calcination at 650 °C were found to be in the range of 60-100 nm. The final crystallite sizes of CaO nano-particles obtained after calcination at 650 °C were found to be in the range of 110-170 nm as seen in Figure C2. The crystallite size of CaO calcination in air leads to the smaller crystallite sizes to compare calcination under vacuum.

Claim 3. Synthesis of metal oxides nanoparticles by calcination in air

3.1. Synthesis of further pure metal oxide nano-particles. To confirm claim 1.1 further, in addition to CaO nano-particles reported in Claim 2, three further types of nano-metal-oxide-particles were successfully synthesized from the list of the 13 possible nano- metal-oxide-particles of Claim 1.1 using the above-described technology and calcination in air (with their average crystallite sizes measured by XRD): Co_3O_4 (18 nm), Fe_2O_3 (16 nm) and NiO (20 nm). TEM micrographs are in good agreement with the crystallite sizes obtained by XRD. The formation of pure and single phases was also confirmed by XRD, as seen in Figure C3.

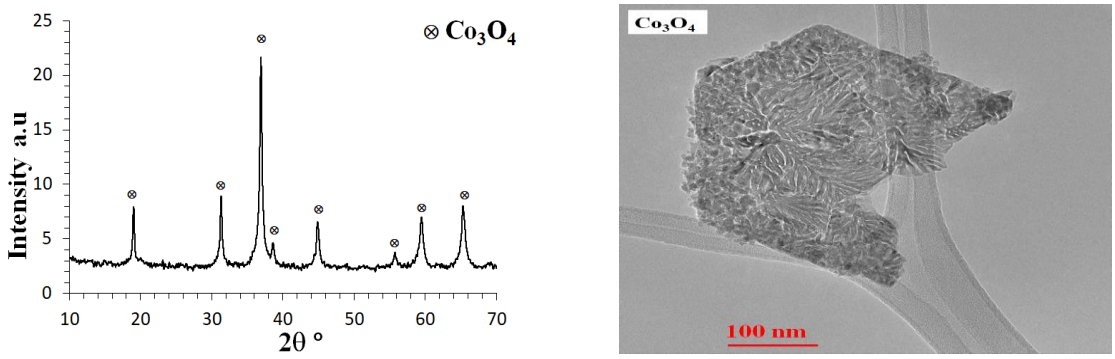

(a)

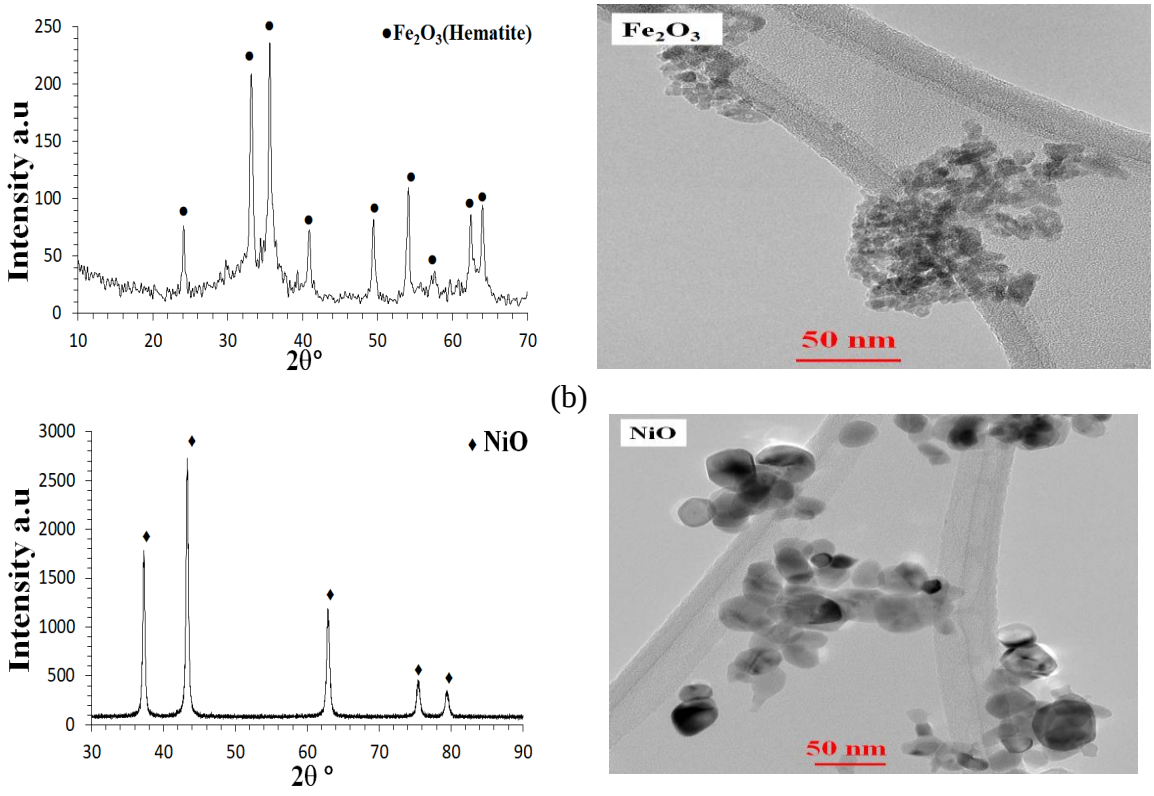

Figure C3: The XRD diffractograms and TEM micrographs of the samples (a) Co_3O_4 (b) Fe_2O_3 (c) NiO

3.2. Synthesis of low-doped CaO. Applying 0.1:1 molar ratio of $NiCl_2$, $CoCl_2$ and $FeCl_3$ to calcium chloride in the initial aqueous solution, low-doped CaO nano-particles were obtained by calcination in air at 650 °C as follows, with their average crystallite sizes: (i) in the 0.1NiO:CaO sample only CaO (42 nm) and NiO (12 nm) phases were detected; (ii) in the 0.1CoO:CaO sample CaO (105 nm) and $Ca_2Co_2O_5$ (50 nm) phases were detected, the latter due to further oxidation of CoO in air and its complex formation with CaO; (iii) in the $0.05Fe_2O_3$:CaO sample CaO (165 nm), Fe_2O_3 (810 nm) and $Ca_2Fe_2O_5$ (14 nm) phases were detected, the latter due to the complex formation of Fe_2O_3 with CaO as seen in Figure C4.

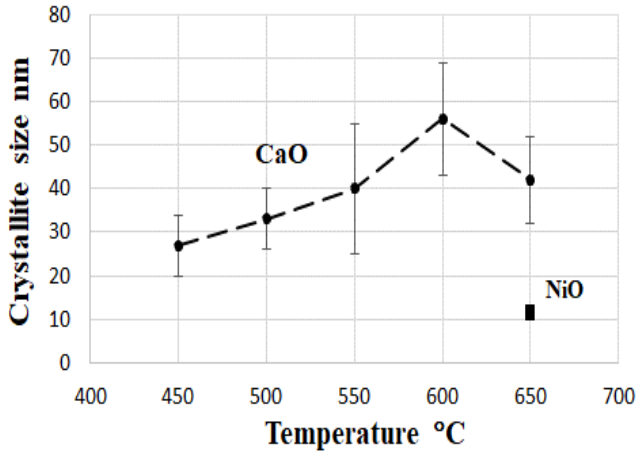

(a)

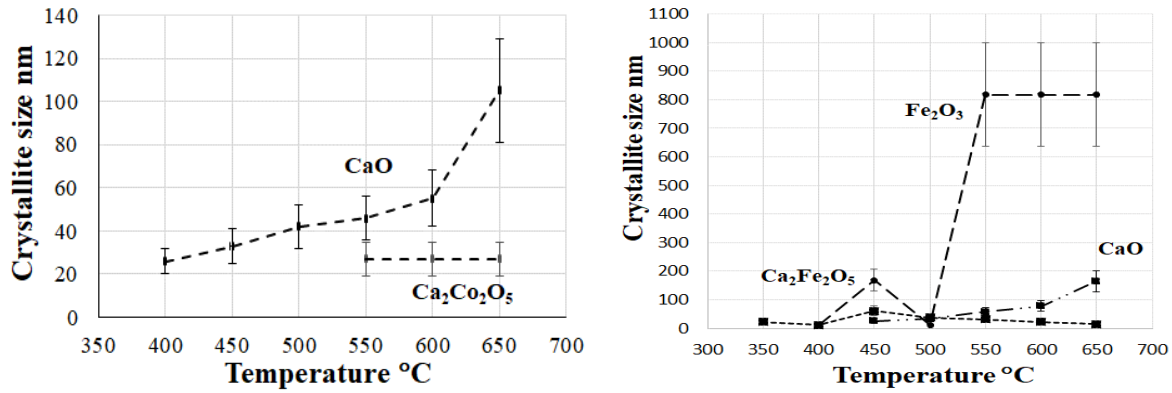

(b) (c)

Figure C4: The crystallite sizes of low-doped CaO as a function of temperatures in the range of 50 - 650 °C (a) 0.1NiO:CaO (b) 0.1CoO:CaO (c) $0.05Fe_2O_3$:CaO

3.3. Synthesis of highly-doped CaO. Applying 0.5:1 molar ratio of $NiCl_2$, $CoCl_2$ and $FeCl_3$ to calcium chloride in the initial aqueous solution, highly doped CaO nanoparticles were obtained by calcination in air at 650 °C as follows, with the average crystallite sizes: (i) in the 0.5NiO:CaO sample only CaO (200 nm) and NiO (20 nm) phases were detected; (ii) in the 0.5CoO:CaO sample CaO (120 nm) and $Ca_2Co_2O_5$ (40 nm) are the major phases; (iii) in the $0.25Fe_2O_3$:CaO sample CaO (820 nm) and $Ca_2Fe_2O_5$ (30 nm) phases were detected as seen in Figure C5.

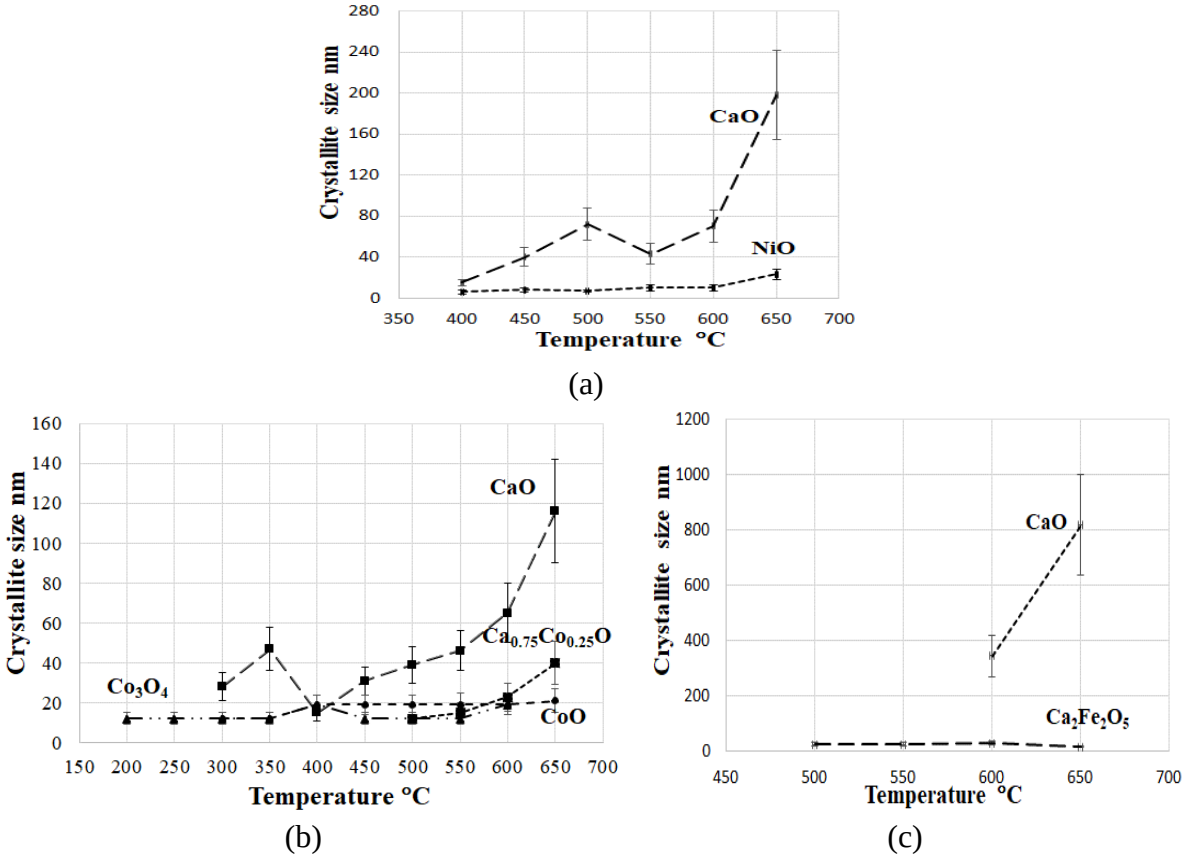

(a)

(b) (c)

Figure C5: The crystallite sizes of low-doped CaO as a function of temperatures in the range of 50 - 650 °C (a) 0.5NiO:CaO (b) 0.5CoO:CaO (c) $0.25Fe_2O_3$:CaO

Claim 4. Carbonation capacity of metal oxide nanoparticles kept in air

4.1. Carbonation capacity of pure CaO nano-particles at room temperature. Pure CaO nano-particles are able to absorb carbon dioxide from normal air at room temperature 25 °C to their full capacity within 450 hours; in this process, the initial pure CaO is fully transformed into $CaCO_3$ and its initial mass is increased to its theoretical maximum by 78 %. Similar (but somewhat lower) results were obtained at 0 °C, as seen in Figure C6.

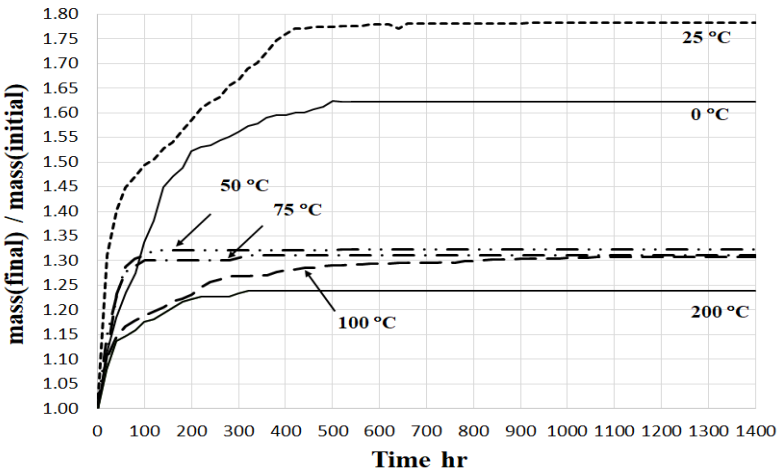

Figure C6: The time dependence of the relative mass change of pure CaO samples exposed to air at different temperatures

4.2. Carbonation capacity of pure CaO nano-particles at higher temperatures. Pure CaO nano-particles at 50 – 75 – 100 – 200 °C were found to absorb much less of carbon dioxide from air compared to room temperature absorption experiments. This was due to the co-absorption of water vapor with the co-formation of $Ca(OH)_2$, blocking the pores in the CaO nano-structure.

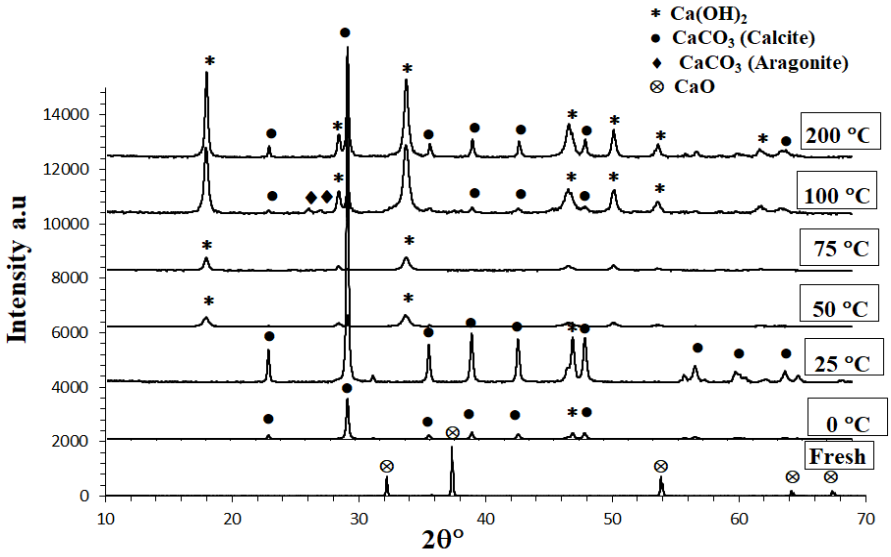

Figure C7: The XRD diffractograms of pure CaO, fresh sample and after the measurements of the sample exposed to air at different temperatures

4.3. The role of doping oxides in carbonation. All doping oxides (NiO, Fe_2O_3 and Co_3O_4) in both low-doped and highly-doped states with CaO were found inactive towards capturing CO_2 or H_2O from normal air in the temperature range of 0 … 200 °C. This was proven by the absence of any peaks for carbonates or hydrates of Ni, Co and Fe in doped CaO samples after they were kept in normal air for hundreds of hours as seen in Figures C8 and C9. In these samples, the same $CaCO_3$ was detected at 0 … 25 °C and additionally, some $Ca(OH)_2$ was found at 50 … 200 °C, as shown above for pure CaO samples. As a result, the carbonation capacity of doped CaO samples was lower compared to pure CaO samples, as the doping oxides had only some diluting effect.

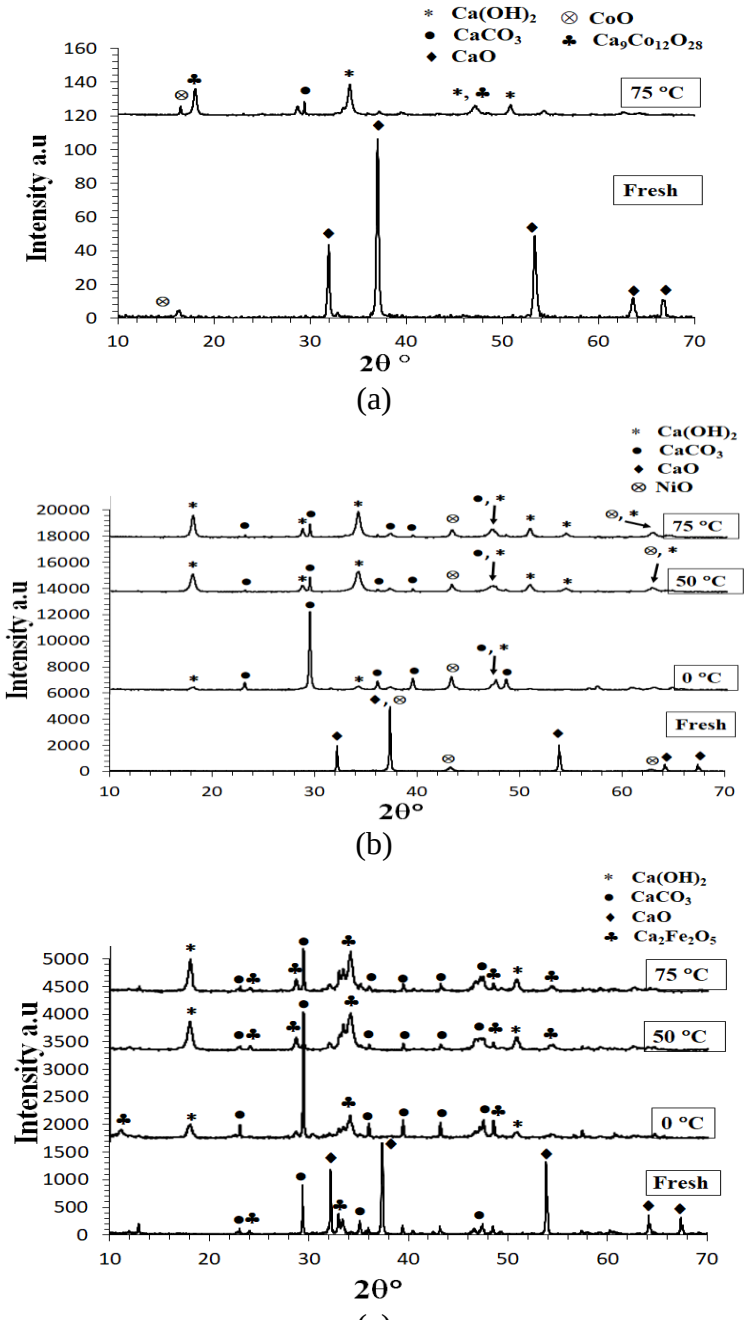

Figure C8: The XRD diffractograms of low-doped CaO fresh sample and after the measurements of the samples exposed to air at different temperatures (a) 0.1CoO:CaO (b) 0.1NiO:CaO and (c) $0.05Fe_2O_3$:CaO

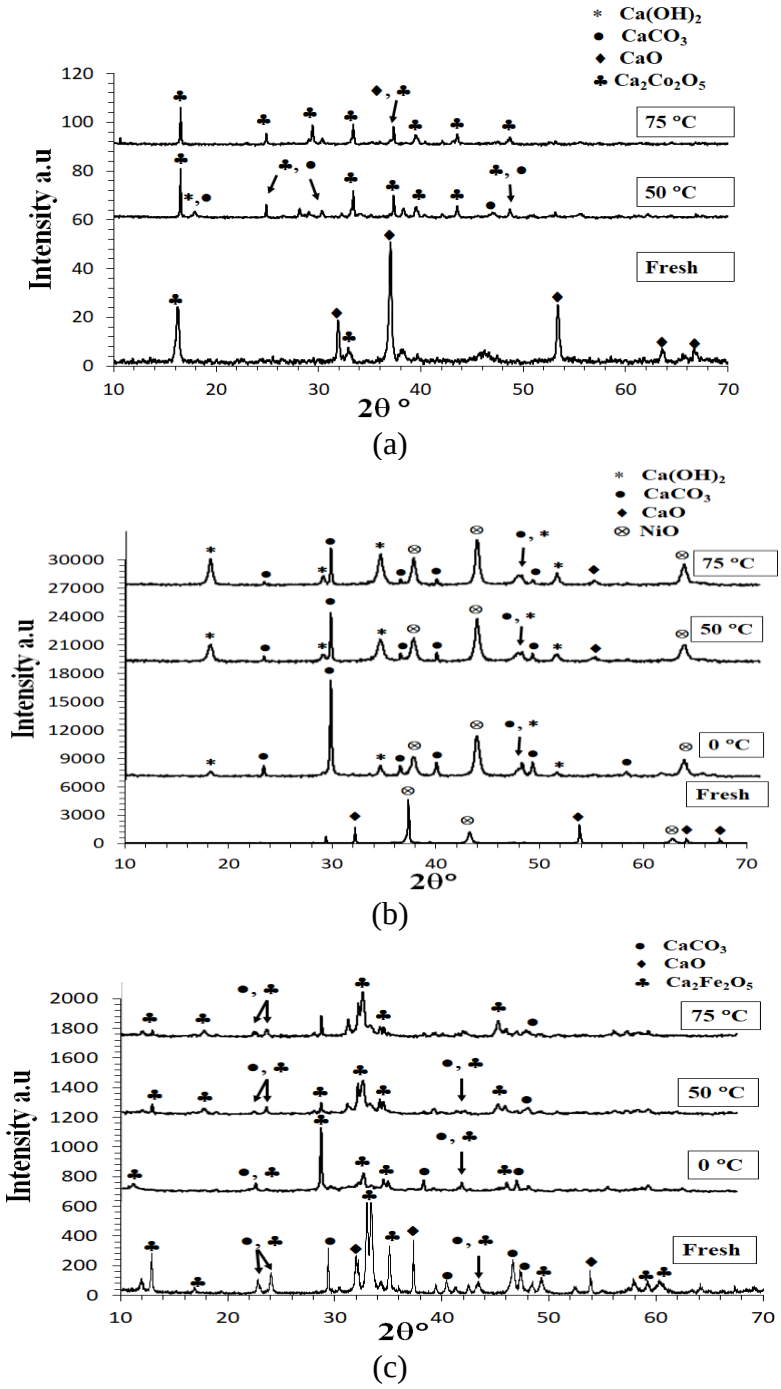

Figure C9: The XRD diffractograms of highly-doped CaO fresh sample and after the measurements of the samples exposed to air at different temperatures (a) 0.5CoO:CaO (b) 0.5NiO:CaO and (c) 0.25Fe_2O_3:CaO

4.4. Final absorbent selection for carbon dioxide capture. Among all nano-metal oxide synthesized and all capturing temperatures studied, pure CaO at 25 °C in air showed the maximum carbon dioxide capturing capacity. Although it takes a longer time (around 450 hours) to fully carbonate pure CaO at 25 °C, it does not require special industrial conditions; capturing of carbon dioxide from normal air will take place slowly but surely by CaO disposed to open fields at a temperature around room temperature.

Acknowledgement

I would like to express my sincere gratitude and appreciation to all these respectful persons. Without them, my PhD journey will not be straightforward to complete. First of all, I would like to express my sincere and deepest appreciation to my supervisors Prof. Dr. George Kaptay and Prof. Dr. Peter Baumli. Their guidance, giving the lectures to fulfil the knowledge and support for my research direction and experimentation made my study journey more academically structured.

Moreover, I would like to thank Dr. Ference Kristaly for his assistance with XRD investigations, giving us lectures on XRD subjects, and especially huge support and suggestions for both my publications and my experimental work. I would like to thank Dr. Andrea Simon, who reviewed my work. I am always thankful to Dr. Anna Sycheva and Dr. Daniel Koncs-Horvath for SEM investigations, Mr. Gabor Karacs for TEM investigations, Mr. Tibor Ferenczi for BET investigations, Dr. Veres Zsolt for helping me to use the furnace.

I would like to express my sincere gratitude to Ms. Agnes Solczi not only for being our faculty coordinator and handling all the administrative work with responsibility but also for her encouragement and support of any inconvenient issues during my entire stay in Hungary. I would like to thank Mrs. Aniko Zoltanne Markus and Mrs. Napsugar Bodnarne Nyari for helping during my experimental work more convenient.

I would like to express my appreciation to Tempus Public Foundation and Stipendium Hungaricum Scholarship Programme for giving me the opportunity to study and providing financial support for my entire stay in Hungary. I would like to extend my gratitude to the Institute of Physical Metallurgy, Metal Forming and Nanotechnology and Antal Kerpely Doctoral School of Materials Science and Technology (Faculty of Material Science and Engineering) at the University of Miskolc. This research work was financed by GINOP2.3.2-15-2016-0027 “Sustainable operation of the workshop of excellence for the research and development of crystalline and amorphous nanostructured materials” project implemented in the framework of Szechenyi 2020 program. The realization of this work was supported by the European Union. I would like to thank the Head of the doctoral school, Professor Dr. Valeria Mertinger, for providing me with the necessary equipment and giving us the lectures for the XRD subject.

I would like to thank both Hungarian and International students for helping and supporting my research work. I would like to thank my close colleagues Jamal Eldin Fadoul Mohammed Ibrahim as well as my seniors Dr. Kanokon Nuilek and Dr. Patcharapon Somedee, who recently graduated, for their encouragement, understanding, and support throughout my PhD journey.

Finally, I am grateful to my parents and my siblings for their continuous support and motivation throughout my entire life.

References

[1] A. Nazari, S. Riahi, S. Riahi, S. Fatemeh Shamekhi, and A. Khademno, "Mechanical properties of cement mortar with Al_2O_3 nanoparticles," J. Am. Sci., vol. 6, no. 4, pp. 94–97, 2009.

[2] S. Stankic, S. Suman, F. Haque, and J. Vidic, "Pure and multi metal oxide nanoparticles: Synthesis, antibacterial and cytotoxic properties," J. Nanobiotechnology, vol. 14, no. 1, pp. 1–20, 2016, doi: 10.1186/s12951-016-0225-6.

[3] L. Habte, N. Shiferaw, D. Mulatu, T. Thenepalli, R. Chilakala, and J. W. Ahn, "Synthesis of nano-calcium oxide fromwaste eggshell by sol-gel method," Sustain., vol. 11, no. 11, pp. 1–10, 2019, doi: 10.3390/su11113196.

[4] M. A. Aseel, F. H. Itab, and F. M. Ahmed, "Producing High Purity of Metal Oxide Nano Structural Using Simple Chemical Method," J. Phys. Conf. Ser., vol. 1032, no. 1, 2018, doi: 10.1088/1742-6596/1032/1/012036.

[5] S. Jha, R. Singh, A. Pandey, and S. Tripathi, "Bacterial Toxicological Assay of Calcium Oxide Nanoparticles against some Plant Growth Promoting Rhizobacteria,"International J for res in applied sci and eng tech(IJRASET),ISSN 2321-9653, vol. 6, no. 11, 2018.

[6] R. Mohadi, K. Anggraini, F. Riyanti, and A. Lesbani, "Preparation Calcium Oxide From Chicken Eggshells," Sriwij. J. Environ., vol. 1, no. 2, pp. 32–35, 2016, doi: 10.22135/sje.2016.1.2.32-35.

[7] Z. X. Tang, D. Claveau, R. Corcuff, K. Belkacemi, and J. Arul, "Preparation of nano-CaO using thermal-decomposition method," Mater. Lett., vol. 62, no. 14, pp. 2096–2098, 2008, doi: 10.1016/j.matlet.2007.11.053.

[8] P. Jamrunroj, S. Wongsakulphasatch, A. Maneedaeng, C. K. Cheng, and S. Assabumrungrat, "Surfactant assisted CaO-based sorbent synthesis and their application to high-temperature CO_2 capture," Powder Technol., vol. 344, pp. 208–221, 2019, doi: 10.1016/j.powtec.2018.12.011.

[9] M. Sadeghi and M. H. Husseini, "A Novel Method for the Synthesis of CaO Nanoparticle for the Decomposition of Sulfurous Pollutant," J. Appl. Chem. Res., vol. 7, no. 4, pp. 39–49, 2013.

[10] A. J. Szalai, N. Manivannan, and G. Kaptay, "Super-paramagnetic magnetite nanoparticles obtained by different synthesis and separation methods stabilized by biocompatible coatings," Colloids Surfaces A Physicochem. Eng. Asp., vol. 568, pp. 113–122, 2019, doi: 10.1016/j.colsurfa.2019.02.006.

[11] J. Gupta and M. Agarwal, "Preparation and characterizaton of CaO nanoparticle for biodiesel production," AIP Conf. Proc., vol. 1724, 2016, doi: 10.1063/1.4945186.

[12] A. Roy and J. Bhattacharya, "Microwave assisted synthesis of CaO nanoparticles and use in waste water treatment " NSTI-Nanotech 2011, vol. 3, no. 1, pp. 565–568, 2011.

[13] Z. X. Tang, Z. Yu, Z. L. Zhang, X. Y. Zhang, Q. Q. Pan, and L. E. Shi, "Sonication-assisted preparation of CaO nanoparticles for antibacterial agents," Quim. Nova, vol. 36, no. 7, pp. 933–936, 2013, doi: 10.1590/S0100-40422013000700002.

[14] S. A. Salaudeen, B. Acharya, and A. Dutta, "CaO-based CO_2 sorbents: A review on screening, enhancement, cyclic stability, regeneration and kinetics modelling," J. CO_2 Util., vol. 23, pp. 179–199, 2018, doi: 10.1016/j.jcou.2017.11.012.

[15] A. Benedetti, J. Ilavsky, C. Segre, and M. Strumendo, "Analysis of textural properties of CaO-based CO_2 sorbents by ex situ USAXS," Chem. Eng. J., vol. 355, pp. 760–776, 2019, doi: 10.1016/j.cej.2018.07.164.

[16] X. Ma, Y. Li, X. Yan, W. Zhang, J. Zhao, and Z. Wang, "Preparation of a morph-genetic CaO-based sorbent using paper fibre as a biotemplate for enhanced CO_2 capture," Chem. Eng. J., vol. 361, no. October 2018, pp. 235–244, 2019, doi: 10.1016/j.cej.2018.12.061.

[17] B. Zhao, L. Ma, H. Shi, K. Liu, and J. Zhang, "Calcium precursor from stirring processes at room temperature for controllable preparation of nanostructure CaO sorbents for high-temperature CO_2 adsorption," J. CO_2 Util., vol. 25, pp. 315–322, 2018, doi: 10.1016/j.jcou.2018.04.012.

[18] A. Granados-Pichardo, F. Granados-Correa, V. Sánchez-Mendieta, and H. Hernández-Mendoza, "New CaO-based adsorbents prepared by solution combustion and high-energy ball-milling processes for CO_2 adsorption: Textural and structural influences," Arab. J. Chem., vol. 13, no. 1, pp. 171–183, 2020, doi: 10.1016/j.arabjc.2017.03.005.

[19] F. Donat and C. R. Müller, "A critical assessment of the testing conditions of CaO-based CO_2 sorbents," Chem. Eng. J., vol. 336, pp. 544–549, 2018, doi: 10.1016/j.cej.2017.12.050.

[20] B. Azimi, M. Tahmasebpoor, P. E. Sanchez-Jimenez, A. Perejon, and J. M. Valverde, "Multicycle CO_2 capture activity and fluidizability of Al-based synthesized CaO sorbents," Chem. Eng. J., vol. 358, pp. 679–690, 2019, doi: 10.1016/j.cej.2018.10.061.

[21] W. Liu et al., "Performance enhancement of calcium oxide sorbents for cyclic CO_2 capture-a review," Energy and Fuels, vol. 26, no. 5, pp. 2751–2767, 2012, doi: 10.1021/ef300220x.

[22] E. Arul, K. Raja, S. Krishnan, K. Sivaji, and S. J. Das, "Bio-Directed Synthesis of Calcium Oxide (CaO) Nanoparticles Extracted from Limestone Using Honey," J. Nanosci. Nanotechnol., vol. 18, no. 8, pp. 5790–5793, 2018, doi: 10.1166/jnn.2018.15386.

[23] D. Kulkarni and I. E. Wachs, "Isopropanol oxidation by pure metal oxide catalysts: Number of active surface sites and turnover frequencies," Appl. Catal. A Gen., vol. 237, no. 1–2, pp. 121–137, 2002, doi: 10.1016/S0926-860X(02)00325-3.

[24] A. R. Butt, S. Ejaz, J. C. Baron, M. Ikram, and S. Ali, "CaO nanoparticles as a potential drug delivery agent for biomedical applications," Dig. J. Nanomater. Biostructures, vol. 10, no. 3, pp. 799–809, 2015.

[25] H. Chen, N. Khalili, and J. Li, "Development of stabilized Ca-based CO_2 sorbents supported by fly ash," Chem. Eng. J., vol. 345, pp. 312–319, 2018, doi: 10.1016/j.cej.2018.03.162.

[26] S. Abraham and V. P. Sarathy, "Biomedical Applications of Calcium Oxide Nanoparticles - A Spectroscopic Study," Int. J. Pharm. Sci. Res., vol. 49, no. 1, pp. 121–125, 2018.

[27] S. M. El-Dafrawy, H. M. Youssef, W. O. Toamah, and M. M. El-Defrawy, “Synthesis of nano-CaO particles and its application for the removal of copper (II), Lead (II), cadmium (II) and iron (III) from aqueous solutions,” Egypt. J. Chem., vol. 58, no. 6, pp. 579–589, 2015, doi: 10.21608/ejchem.2015.1007.

[28] M. M. Durano, A. H. Tamboli, and H. Kim, “Cobalt oxide synthesized using urea precipitation method as catalyst for the hydrolysis of sodium borohydride,” Colloids Surfaces A Physicochem. Eng. Asp., vol. 520, pp. 355–360, 2017, doi: 10.1016/j.colsurfa. 2017.02.005.

[29] K. Phiwdang, S. Suphankij, W. Mekprasart, and W. Pecharapa, “Synthesis of CuO nanoparticles by precipitation method using different precursors,” Energy Procedia, vol. 34, pp. 740–745, 2013, doi: 10.1016/j.egypro.2013.06.808.

[30] A. Aimable, M. T. Buscaglia, V. Buscaglia, and P. Bowen, “Polymer-assisted precipitation of ZnO nanoparticles with narrow particle size distribution,” J. Eur. Ceram. Soc., vol. 30, no. 2, pp. 591–598, 2010, doi: 10.1016/j.jeurceramsoc.2009.06.010.

[31] K. Sinkó, G. Szabó, and M. Zrínyi, “Liquid-phase synthesis of cobalt oxide nanoparticles,” J. Nanosci. Nanotechnol., vol. 11, no. 5, pp. 4127–4135, 2011, doi: 10.1166/jnn.2011.3875.

[32] A. Hakim et al., “Studies on CO_2 Adsorption and Desorption Properties from Various Types of Iron Oxides (FeO, Fe_2O_3, and Fe_3O_4),” Ind. Eng. Chem. Res., vol. 55, no. 29, pp. 7888–7897, 2016, doi: 10.1021/acs.iecr.5b04091.

[33] J. B. Holquist and D. M. Klaus, “Characterization of potassium superoxide and a novel packed bed configuration for closed environment air revitalization." 44th International Conference on Environmental Systems 2014. http://hdl.handle.net/2346/59647.

[34] A. A. Peyghan and S. Yourdkhani, “Capture of carbon dioxide by a nanosized tube of BeO: A DFT study,” Struct. Chem., vol. 25, no. 2, pp. 419–426, 2014, doi: 10.1007/s11224-013-0307-0.

[35] Y. Duan, D. C. Sorescu, and D. Luebke, “Efficient theoretical screening of solid sorbents for CO2 capture applications,” International Journal of Clean Coal and Energy, vol.1, no. NETL-PUB-318, pp. 661–677, 2011. doi.org/10.4236/ijcce.2012.11001

[36] H. A. Mosqueda, C. Vazquez, P. Bosch, and H. Pfeiffer, “Chemical sorption of carbon dioxide (CO2) on lithium oxide (Li2O),” Chem. Mater., vol. 18, no. 9, pp. 2307–2310, 2006, doi: 10.1021/cm060122b.

[37] J. Ortiz-Landeros, T. L. Ávalos-Rendón, C. Gómez-Yáñez, and H. Pfeiffer, “Analysis and perspectives concerning CO_2 chemisorption on lithium ceramics using thermal analysis,” ournal of thermal analysis and calorimetry, vol. 108, no. 2, pp. 647–655, 2012, doi: 10.1007/ s10973-011-2063-y.

[38] W. N. R. Wan Isahak, Z. A. C. Ramli, M. W. Mohamed Hisham, and M. A. Yarmo, “Magnesium oxide nanoparticles on green activated carbon as efficient CO_2 adsorbent,” AIP Conf. Proc., vol. 1571, no. 1, pp. 882–889, 2013,2013. doi: 10.1063/1.4858766.

[39] Y. Duan and D. C. Sorescu, “CO_2 capture properties of alkaline earth metal oxides and hydroxides: A combined density functional theory and lattice phonon dynamics study,” J. Chem. Phys., vol. 133, no. 7, 2010, doi: 10.1063/1.3473043.

[40] Y. D. Ding, G. Song, X. Zhu, R. Chen, and Q. Liao, "Synthesizing MgO with a high specific surface for carbon dioxide adsorption," RSC Adv., vol. 5, no. 39, pp. 30929–30935, 2015, doi: 10.1039/c4ra15127e.

[41] M. Bhagiyalakshmi, J. Y. Lee, and H. T. Jang, "Synthesis of mesoporous magnesium oxide: Its application to CO_2 chemisorption," Int. J. Greenh. Gas Control, vol. 4, no. 1, pp. 51–56, 2010. doi: 10.1016/j.ijggc.2009.08.001.

[42] T. S. Marliza, M. A. Yarmo, A. Hakim, M. N. A. Tahari, M. W. M. Hisham, and Y. H. Taufiq-Yap, "CO_2 capture on NiO supported imidazolium-based ionic liquid," AIP Conf. Proc., vol. 1838, no. 1, p. 020008, 2017, doi: 10.1063/1.4982180.

[43] I. Yanase, S. Konno, and H. Kobayashi, "Reversible CO_2capture by ZnO slurry leading to formation of fine ZnO particles," Adv. Powder Technol., vol. 29, no. 5, pp. 1239–1245, 2018. doi: 10.1016/j.apt.2018.02.016.

[44] S. Kumar, "The effect of elevated pressure, temperature and particles morphology on the carbon dioxide capture using zinc oxide," J. CO_2 Util., vol. 8, pp. 60–66, 2014, doi: 10.1016/j.jcou.2014.07.002.

[45] Z. Mirghiasi, F. Bakhtiari, E. Darezereshki, and E. Esmaeilzadeh, "Preparation and characterization of CaO nanoparticles from $Ca(OH)_2$ by direct thermal decomposition method," J. Ind. Eng. Chem., vol. 20, no. 1, pp. 113–117, 2014, doi: 10.1016/ j.jiec. 2013.04.018.

[46] T. Nimmas et al., "Influence of CaO precursor on CO_2 capture performance and sorption-enhanced steam ethanol reforming," Int. J. Hydrogen Energy, vol. 44, no. 37, pp. 20649–20662, 2019, doi: 10.1016/j.ijhydene.2018.07.095.

[47] D. Karami and N. Mahinpey, "Highly active CaO-based sorbents for CO_2 capture using the precipitation method: Preparation and characterization of the sorbent powder," Ind. Eng. Chem. Res., vol. 51, no. 12, pp. 4567–4572, 2012. doi: 10.1021/ie2024257.

[48] A. R. Butt, S. Ejaz, J. C. Baron, M. Ikram, and S. Ali, "CaO nanoparticles as a potential drug delivery agent for biomedical applications," Dig. J. Nanomater. Biostructures, vol. 10, no. 3, pp. 799–809, 2015.

[49] H. Guo, S. Yan, Y. Zhao, X. Ma, and S. Wang, "Influence of water vapor on cyclic CO_2 capture performance in both carbonation and decarbonation stages for Ca-Al mixed oxide," Chem. Eng. J., vol. 359, pp. 542–551, 2019, doi: 10.1016/j.cej.2018.11.173.

[50] H. J. Yoon and K. B. Lee, "Introduction of chemically bonded zirconium oxide in CaO-based high-temperature CO_2 sorbents for enhanced cyclic sorption," Chem. Eng. J., vol. 355, pp. 850–857, 2019, doi: 10.1016/j.cej.2018.08.148.

[51] F. He, H. Wang, and Y. Dai, "Application of Fe_2O_3/ Al_2O_3 Composite Particles as Oxygen Carrier of Chemical Looping Combustion," J. Nat. Gas Chem., vol. 16, no. 2, pp. 155–161, 2007, doi: 10.1016/S1003-9953(07)60041-3.

[52] P. Wang and I. M. C. Lo, "Synthesis of mesoporous magnetic γ-Fe_2O_3 and its application to Cr(VI) removal from contaminated water," Water Res., vol. 43, no. 15, pp. 3727–3734, 2009, doi: 10.1016/j.watres.2009.05.041.

[53] S. W. Cao, Y. J. Zhu, M. Y. Ma, A. Li, and L. Zhang, "33Hierarchically nanostructured magnetic hollow spheres of Fe_3O_4 and γ-Fe_2O_3: Preparation and potential application in drug delivery," J. Phys. Chem. C, vol. 112, no. 6, pp. 1851–1856, 2008, doi: 10.1021/ jp077468.

[54] L. Di Felice, C. Courson, P. U. Foscolo, and A. Kiennemann, "Iron And Nickel Doped Alkaline-Earth Catalysts For Biomass Gasification With Simultaneous Tar Reformation And CO_2 Capture," Int. J. Hydrogen Energy, vol. 36, no. 9, pp. 5296–5310, 2011, doi: 10.1016/ j.ijhydene.2011.02.008.
[55] D. R. Lide, CRC Handbook of Chemistry and Physics. 2005.
[56] I. Barin, Thermochemical Data of pure substances, Second. New York, 1993.

Publications related to this research work

Journal papers

1. E. E. Khine et al., "Preparation of calcium oxide by a precipitation method," Material Science and Engineering, vol. 45, no. 1, pp. 182–190, 2020. DOI: 10.32974.mse.2020.018
2. E. E. Khine et al., "Synthesis and characterization of calcium oxide nanoparticles for CO_2 capture," J. Nanoparticle Res., vol. 24, no. 7, 2022, doi: 10.1007/s11051-022-05518-z. (Q2)

Proceeding papers

1. E. E. Khine et al., "Synthesis of new Fe_2O_3 doped CaO nanoparticles via precipitation method and their characterizations". Proceeding of the 1 st International Congress on Modern Sciences Tashkent Chemical-Technologies Institude conference, May10-11,2022, Uzberkistan, ISBN: 978-625-7464-90-1.
2. E. E. Khine et al., "Pure CaO and Fe_2O_3 nanoparticles calcined under vacuum: preparations and characterizations". Proceedings of 6^{th} International Asian Congress on Contemporary Science VI Conference, May27-29, 2022, Van, Turkey.